Low-temperature spectroscopic studies of single molecules in 3-D and on 2-D hosts

Smit, R.

1

INTRODUCTION TO SINGLE-MOLECULE SPECTROSCOPY

1.1. LOW-TEMPERATURE SPECTROSCOPY

1.1.1. LINE-NARROWING SPECTROSCOPY

The discovery of liquid helium in 1908 by Leiden's Heike Kamerlingh Onnes fueled a plethora of experiments that has led to today's status of the field of low-temperature spectroscopy. Four decades after Heike's discovery, the Russian scientist Eduard Shpol'skii observed that fluorescent aromatic molecules frozen into *n*-alkane crystals showed significant line narrowing in the absorption and emission spectra at liquid-helium temperatures, which made it possible to study the vibrational and electronic structure of molecules. His method became known as Shpol'skii spectroscopy.[1,2] Since then, the bases of the experiments have not changed considerably. The experiments on single molecules still require a host matrix that can be doped with fluorescent molecules to induce immobilization of the otherwise rapidly-diffusing molecules. Although the spectroscopy of ensembles of molecules in solids became very common, it took a couple of decades before the signal of a single molecule was detected in a host medium, namely in 1989 by W.E. Moerner[3] and 1990 by M. Orrit,[4] both for single pentacene molecules in a *p*-terphenyl host matrix. The ensemble-average-free detection method found by Orrit is today still the dominant method, namely through their emitted fluorescence signal. Nowadays, single-molecule spectroscopy, not restricted to low temperature, has developed into a broad field of research, stretching from applications in the sub-diffraction-limited imaging of (bio)structures through super-resolution microscopy,[5] applications in quantum optics[6] up to employing molecules for sensing at the nanoscale (see section 1.1.4).

The fluorescent molecules that are studied in low-temperature spectroscopy generally belong to the class of polycyclic aromatic hydrocarbons, which includes molecules such

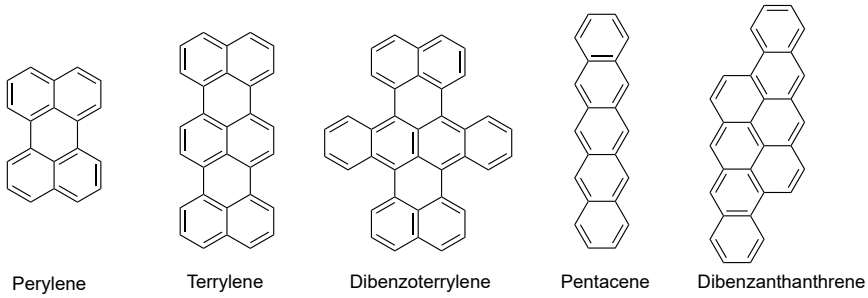

Figure 1.1.: Chemical structures of the most-used fluorescent molecules in low-temperature single-molecule spectroscopy.

as perylene, terrylene, pentacene, dibenzoterrylene and dibenzanthanthrene (see chemical structures in Figure 1.1. These molecules are typically studied inside aromatic host matrices such as anthracene, naphthalene or *p*-terphenyl. Apart from these three host matrices there are many more, but the number of guests molecules is rather limited, as they require favorable spectroscopic properties, such as a strong and stable fluorescence output. A schematic energy level structure of a guest molecule, embedded into a solid host, is depicted in Figure 1.2. First of all, there are the electronic states of the molecule, which are the singlet ground (S_0) and singlet excited state (S_1), usually separated by 1.5-3 eV, corresponding to the region of visible light. Another excited state exists in between the two singlets, which is the triplet state (T_1) and consists, as its name implies, of three sublevels with the three allowed spin quantum numbers, as total spin amounts to 1. Coupled to these electronic states are the molecular vibrations, which have energies in the order of 30-300 meV. In addition, since the molecule is in a solid medium, the electronic states also couple to low-frequency modes or phonons, which are typically low energy bands (up to 10-20 meV in bandwidth). A transition between the singlet ground and singlet excited state is highly allowed and does not violate spin or parity selection rules. Since it is highly allowed, the decay rate is also fast and typically in the order of nanoseconds. This decay can involve two processes, namely through excitation of multiple vibrational quanta, called internal conversion, or the emission of a photon, leading to fluorescence. For highly-fluorescent molecules, the radiative decay rate largely exceeds the internal conversion or non-radiative decay rate, yielding a high quantum yield of fluorescence. The molecules depicted in Figure 1.1 all have a high fluorescence quantum yield.

A transition from the singlet to the triplet is spin-forbidden, as one of the electrons has to flip a spin. However, the transition can occur with a very low probability through intersystem crossing (ISC) and is a combination of a spin-flip and internal conversion (blue and red dashed arrow in Figure 1.2). Once the molecule is in the triplet state it cannot emit fluorescence anymore and this leads to quantum jumps in the fluorescence.[7] The blinking can for some molecules extend to a relatively long time scale of milliseconds up to seconds (see for example the triplet state of dibenzothiophene

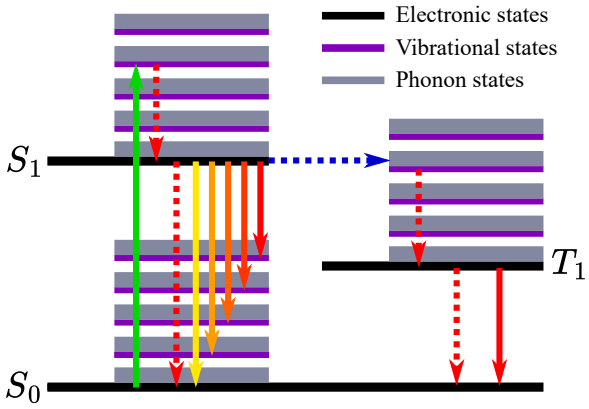

Figure 1.2.: Jablonski diagram of the three-level system of an aromatic molecule. The black bars indicate the electronic states, the purple bars the vibrational states and grey bars indicate the phonon bands. Excitation to one of the vibrational levels in the electronic excited state leads to quick dissipation of the vibrational energy. From there, the molecule can decay into one of the vibrational and/or phonon states, leading to red-shifted emission, or non-radiatively decay into the triplet state (intersystem crossing). Both pathways lead eventually back to the ground state singlet. Non-radiative processes are indicated by a dashed red arrow, intersystem crossing by a blue dashed arrow and processes involving the absorption or emission of a photon are given by a solid arrow.

in Chapter 3). The decay back to the ground state is often dominated by non-radiative decay instead of the emission of a photon, for which the latter process is called phosphorescence (see phosphorescence studies in Chapter 3). For most of the molecules in Figure 1.1, the triplet yield through intersystem crossing is very low: its probability is in the order of $10^{-6} - 10^{-7}$ per excitation. Hence, these molecules can be effectively described as two-level systems. In case the molecule remains only shortly in the triplet state, such as applies to dibenzoterrylene (around 40 µs[8]), the overall loss of fluorescence, due to infrequent visits to the triplet state, is also limited, leading to a very stable fluorescence signal. In Chapter 2, I will show a process that can partly overcome fluorescence loss by ISC, namely through the inverse of ISC, called reverse intersystem crossing.

The fluorescence occurs by cycles through the two singlet states, shown in Figure 1.2, when continuously excited with a light source whose photon energy matches the transition's energy gap, i.e. is resonant with the transition. Resonant photons can excite the molecule to either the purely electronic state or some vibrational state. An excited vibrational state is usually short-lived, with typical lifetimes of (tens of) picoseconds[9] and therefore we end up in the vibrational ground state of the excited singlet. It is also possible to excite to a higher singlet state, but the internal conversion would

again quickly relax the molecule back to the first excited singlet, a process known as Kasha's rule[10] (with some notable exceptions, such as Azulene[11]). After relaxation, the molecule falls back to the ground state and emits a photon. The decay can excite one (or more) vibration(s), either a molecular vibration and/or phonon, which translates into an energy loss of the photon and leads to red-shifted emission. In case the electronic states of the molecule couple weakly to the phonon states of the medium, we obtain a fluorescence emission spectrum that consists of zero-phonon lines (ZPL) with weak phonon side bands (Figure 1.3). The zero-phonon lines correspond to emission from the purely electronic transition (called the 0-0 zero-phonon line) and emission into any of the vibrational states (0-N zero-phonon line for the N-th vibrational state).

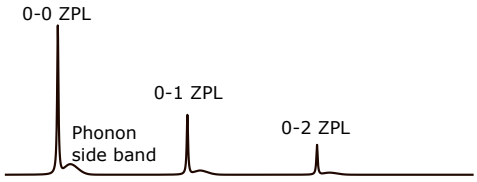

Figure 1.3.: Schematic fluorescence emission spectrum with the purely electronic transition (0-0 ZPL) and two red-shifted peaks that are due to an additional excitation of a vibrational state. Next to the ZPL peaks there are weak phonon side bands.

The intensity of the phonon side band compared to emission into the 0-0 ZPL depends on the strength of the electron-phonon coupling of the host-guest system. A careful choice of the host can give rise to weak phonon side bands in the spectrum. A typical number used for describing the intensity of the phonon side bands is the Debye-Waller factor $\alpha_{DW} = I_{ZPL}/(I_{ZPL} + I_{PSB})$. In the best host/guest systems this value can be up to 0.9. The intensity of the vibrational peaks, the 0-N ZPLs, is for the most part a property of the molecule itself and does not vary significantly by host. It relies on the coupling of the ground state vibrational wavefunction, in the excited electronic state, to the vibrational wavefunctions coupled to the ground electronic state. This is governed by overlap integrals, which are called the Franck-Condon factors. These overlap integrals determine the weights of the 0-N ZPLs in the fluorescence emission spectrum. The sum of these Franck-Condon factors compared to the intensity of the 0-0 ZPL, will be called α_{FC}. The total emission into the 0-0 ZPL as compared to the whole spectrum is the product of α_{DW} and α_{FC}, sometimes denoted as the branching ratio. In best cases, branching ratios of up to 0.55 have been found for dibenzoterrylene in *p*-terphenyl.[12] The high branching ratios for dibenzoterrylene have made this a model molecule for studies in quantum optics, which aim to employ single molecules as single photon sources, with high photon indistinguishably (scales with branching ratio).[13] In Chapter 5, an unconventional host matrix for terrylene is studied, namely two-dimensional hexagonal boron nitride, in which it is possible to find molecules with branching ratios that exceed record values that have been found for (dibenzo)terrylene in other host matrices.

1.1.2. THE 0-0 ZERO-PHONON LINE (ZPL)

In low-temperature single-molecule spectroscopy, the focus is usually on the narrow purely-electronic transition or the 0-0 ZPL. The width of this line is determined by quantum mechanics and is derived from Heisenberg's uncertainty relation:

$$\Gamma_0 = \frac{1}{\pi T_2} = \frac{1}{2\pi T_1} + \frac{1}{\pi T_2^*}. \tag{1.1}$$

The quantity T_1 is the excited state lifetime and T_2 is the decoherence time, which is essentially the time scale over which the molecule can be considered as not interacting with the environment and is left unperturbed. At best, the decoherence time is twice T_1, the timescale at which the excited state (spontaneously) decays. Any other interactions with the environment, that are occurring on a faster time scale than the excited state lifetime, will lead to additional decoherence. This is captured by T_2^*, which compared to twice T_1, decreases the coherence time and broadens the linewidth. This is for example the source of linewidth broadening that occurs at higher than liquid-helium temperatures, when phonons are populated and with their motion are perturbing the environment around the molecule. However, if all decoherence mechanisms are eliminated, for example phonons are depopulated, the linewidth can reach its minimum set by equation 1.1, called the lifetime (or Fourier) limit. In the case of molecules, with lifetimes in the order of a few ns, the lifetime-limited linewidth is on the order of few tens of MHz and is presented as the full-width-at-half-maximum of a Lorentzian line shape of the resonance. For comparison, at room temperature the linewidths are typically few tens of THz.[12] Hence, the million times narrower linewidth at low temperature becomes very sensitive to quantum effects that can change the resonance's energy, caused for example through coupling to weak (static) fields. The narrow width of the 0-0 ZPL is therefore a useful tool to perform sensing at the nanoscale. In fact, 0-0 ZPLs of many molecules can be used as nano sensors at the same time, due to existence of inhomogeneous broadening.

1.1.3. INHOMOGENEOUS BROADENING

As a molecule is very sensitive to its environment in the host matrix, the inhomogeneity of the environment among many molecules can shift the electronic transition noticeably when compared to the (homogeneous) linewidth of the molecule itself. In real-world non-ideal host crystals there are always impurities, disorder and boundaries in the crystallinity, different isotopes and other mechanisms that lead to a different environment from molecule to molecule. The many molecules with lifetime-limited linewidths, but slightly shifted in energy, that can be present inside a diffraction-limited laser spot of typically 1 μm in width, lead to the formation of a much broader band of fluorescence, called the inhomogeneous band. In typical crystals this band extends from 10-100 GHz in width (see Figure 1.4b), but can be less than 1 GHz broad for extremely pure single crystals.[14] By reducing the concentration of molecules, single molecules can have resonances that are isolated within the inhomogeneous distribution. With a narrow-linewidth tunable laser these molecules can be selectively excited, through their Lorentzian resonances as shown in Figure 1.4a and 1.4c.

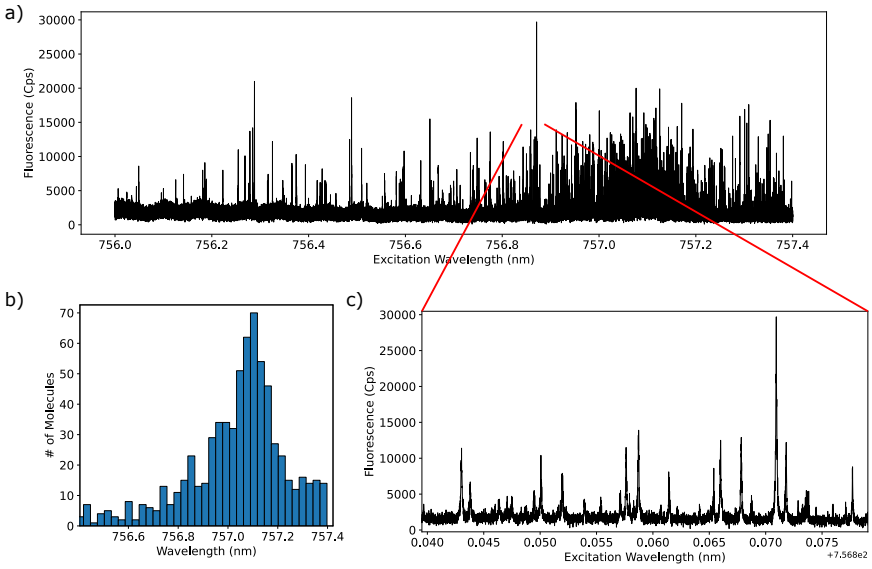

Figure 1.4.: Panel (a) shows a 1.4 nm wide scan of an excitation laser that reveals resonances of single molecules at different wavelengths, detected by the red-shifted fluorescence of dibenzoterrylene molecules in a 2,3-dibromonaphthalene crystal. In panel (b) the positions of the molecules are plotted by incidence into a histogram and reveals the inhomogeneous distribution around a center wavelength of 757.1 nm, with a width of about 0.2 nm (approximately 100 GHz). Panel (c) shows a small segment of the scan corresponding to the area between the two red lines and shows more clearly the Lorentzian line shapes of the resonances from the single molecules. The horizontal axis displays the difference in wavelength with respect to 756.8 nm.

1.1.4. NANOSENSING

Each single molecule within the inhomogeneous broadening is a potential sensor for effects on the nanoscale. One such frequently-studied effect is the Stark effect, which arises due to coupling of the electronic states with an electric field. The shift of the optical resonance itself becomes apparent when the electronic states do not shift equally, increasing or decreasing the singlet energy gap (Figure 1.5a). This difference in frequency can be expressed in the first two orders of perturbation theory as:

$$h\Delta\nu = -\Delta\vec{\mu}.\vec{E} - \frac{1}{2}\vec{E}.\Delta \overleftrightarrow{\alpha} .\vec{E}, \tag{1.2}$$

where $\Delta\vec{\mu}$ (a vector) is the difference in permanent dipole moment between ground and excited state and likewise $\Delta \overleftrightarrow{\alpha}$ (a tensor) is the difference in polarizability between

ground and excited state. The first term is called the linear Stark effect and the second is called the quadratic Stark effect. If the molecule is centrosymmetric and the environment of the molecule leaves this centrosymmetry unchanged, then the quadratic term will be dominant. However, with the quadratic Stark effect the molecule can in most cases only shift downward in frequency, due to a higher polarizability in the excited state, and the shift typically becomes noticeable at strong electric fields of more than 10 kV/cm. That the overall shift can be very large was for instance observed for dibenzoterrylene in anthracene, where the molecules could be shifted by more than 400 GHz.[15] In case the centrosymmetry is broken (see Chapter 4), the linear Stark effect can dominate in equation 1.2. Even at relatively weak electric fields, a large shift of the resonance line can be obtained. A linear Stark shift coefficient of 1.5 GHz/kVcm^{-1} was for example observed for dibenzoterrylene in a 2,3-dibromonaphthalene matrix.[16] Although this shift is strong enough to detect the field of a single charge,[17] the coupling of a single charge to a single molecule remains to be demonstrated.

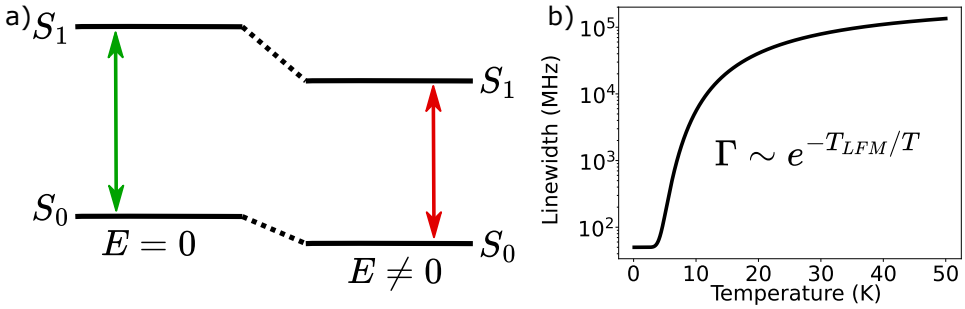

Figure 1.5.: Panel (a) shows the principle of the Stark effect. A nonzero electric field on the right side of the panel leads to shifts of both the ground and excited state singlet. When they shift by a different amount, the energy gap between the levels reduces (or may increase if a difference in dipole is present), leading to a noticeable shift of the optical resonance. Panel (b) shows schematically the line broadening observed in many organic matrices. The broadening is purely induced by decoherence through the population of (low-frequency) phonons and follows an Arrhenius law, shown in the displayed equation. The onset of the broadening is determined by phonon energies of the guest/host system, typically captured by the effective temperature of activation of low-frequency phonon modes (LFMs). This effective temperature is for organic matrices usually in the order of 40 K.[18]

In the past years, the Stark effect has been used for example to study the dipole-dipole coupling between two molecules whose resonances were shifted on top of each other and were spatially separated by less than 20 nm.[19] In other cases, the Stark effect was used to create a single-molecule tunable light source in order to perform spectroscopy on the fine structure of a sodium vapor.[20] In another work it was found that in some

cases a persistent Stark shift could be obtained by using an off-resonant light source with a high intensity, likely causing separation of charges within the host crystal.[21]

Apart from the Stark effect, other sensing applications are for example strain. An experiment with an anthracene crystal mounted on top of a tuning fork displayed line broadening when the tuning fork was excited at resonance.[22] A recent work showed that single molecules can also be used as sensitive thermometers at low temperature by measuring the linewidth as a function of temperature for calibration purposes.[23] The linewidths of single molecules typically broadens with an Arrhenius law due to pure phonon-induced decoherence and is shown schematically in Figure 1.5b. However, there might be additional broadening mechanisms available, namely due to tunneling two-level systems, which will be introduced in the next section and are also studied in Chapter 5.

1.1.5. TUNNELING TWO-LEVEL SYSTEMS

In some cases, molecules are sensing perturbations in their environment that are not intentionally activated. These can occur from dynamics inside the host crystal or around it (adsorbents). The model is typically described as a group of atoms tunneling between two spatial positions, the so-called tunneling two-level systems (TLSs), represented by a double well potential, schematically shown in Figure 1.6. They occur frequently in poorly-crystallized systems, such as glasses, and can explain the additional heat capacity that exists in these materials.[24] Even at the low temperatures that we work at, the TLSs can be active and couple to the molecule's resonance. This leads to spectral jumps and/or fast spectral diffusion,[25] in the case there are many of these TLSs. In well-crystallized systems, these TLSs are generally not present or minimally present. The presence of TLSs has also consequences on the typical broadening curve shown in Figure 1.5b. In general, the activation of TLSs by increasing temperature leads to additional broadening of the linewidth, in the form of a linear term added to the equation in Figure 1.5b. Apart from molecular crystals, TLSs are still subject to intensive study for quantum devices that contain superconducting qubits, as they are a primary source of decoherence for these type of qubits.[26]

1.1.6. TRIPLET STATES

Although most of the spectroscopic measurements are performed on singlet states, the triplet states can be used as sensors as well. Triplet states are not only highly sensitive to their environment, but also to the inner structure of the molecule itself, namely its isotopic composition. As the triplet states often do not provide any measurable signal – phosphorescence is extremely weak – they have to be measured indirectly in the fluorescence signal. A common way to do that is by a scheme called optically-detected magnetic resonance (ODMR, see Figure 1.7). In order to understand this scheme we have to first consider the triplet sublevels. The three triplet sublevels are denoted as T_x, T_y and T_z.[27] In general, the two states T_x and T_y have similar lifetimes and are therefore difficult to separate from each other in measurements of quantum jumps in fluorescence. However, the state T_z typically has a longer lifetime. As the molecule cycles through the singlet states through continuous excitation, it naturally

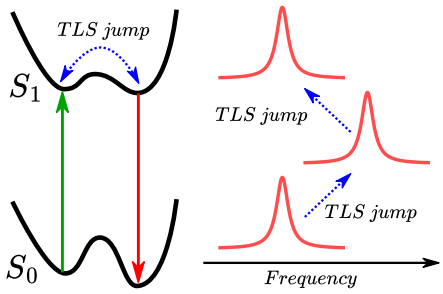

Figure 1.6.: Schematic of the standard model for tunneling two-level systems. The TLS is represented by a double-well potential of possibly two conformational states of a 'group of atoms'. The TLS couples to the optical transition of the molecule and this may induce a jump from one to the other conformation, leading to a frequency shift of the optical transition. The TLSs are typically observed as single discrete jumps. In the case of many two-level systems discrete jumps are not observed anymore and the optical resonance will rather display spectral diffusion. Moreover, TLSs can couple to each other and a jump in one of them can induce a jump in the other.

populates these triplet sublevels levels through intersystem crossing, leading to loss of fluorescence signal. On average, the signal is therefore weaker than what it could have been without intersystem crossing. This loss is especially influenced by the longer lived T_z state and therefore shifting the triplet population from T_x or T_y to T_z will lead to more fluorescence loss. Shifting this population can be done with microwaves that are resonant with the corresponding transitions.[28] This resonance exists due to the zero-field splitting present between the sublevels. Moreover, the splitting can be modified by an external magnetic field due to the Zeeman effect and that makes the triplet sublevels sensitive probes for (local) magnetic fields. In addition, the triplet states couple to any other spins in their environment and most strongly to the spins present within the molecule itself. That can be for instance a nuclear spin of a carbon-13 isotope[29] or single hydrogen nuclei present in the molecule.[30] Experiments in the past showed that it was possible to even reveal at what site a particular isotope was most likely located.[31] Moreover, the triplets are very sensitive to proton spins, for example the hydrogens that terminate the molecule. Replacing these hydrogens by deuterium reduces the hyperfine coupling thanks to the deuterium's six times weaker gyromagnetic ratio as compared to hydrogen. As a consequence the observed resonances of the triplet in ODMR can be as narrow as 100 kHz. However, reaching lifetime-limited linewidths at standard liquid-helium temperatures is impossible, as other spins, such as the hydrogens or deuteriums and natural abundance of carbon-13 (1.1%), are always present in the molecule's inner and outer environment. The coupling of these nuclear spins are responsible for the assymetric lineshape observed in the ODMR spectra as their random flipping narrows the energy gap between $T_y - T_z$, while broadening the

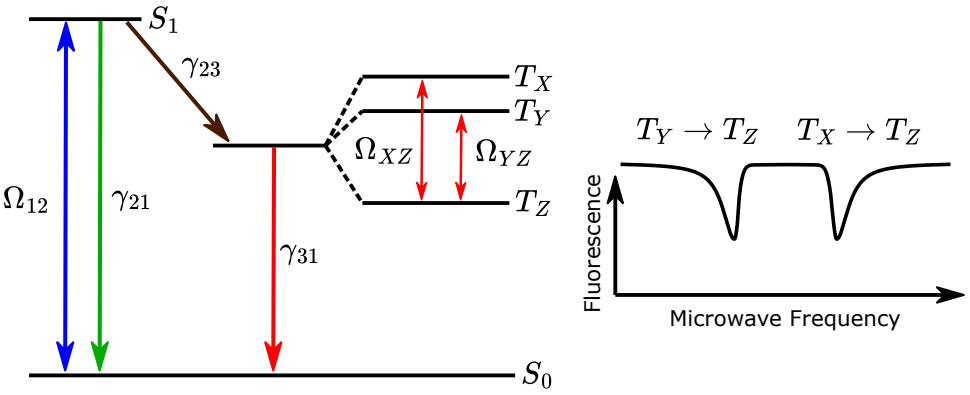

Figure 1.7.: Schematic of the optically-detected magnetic resonance experiment on a single molecule. A laser is in resonance with the singlet transition (Rabi frequency Ω_{12}) inducing fluorescence (with decay rate γ_{21}). With low probability the molecule decays into the triplet state through intersystem crossing (rate γ_{23}) and populates one of the three sublevels that are slightly apart from each other in frequency due to zero-field splitting. With a microwave that is resonant with transitions between the sublevels (with Rabi frequencies Ω_{XZ} and Ω_{YZ}), the population can be transferred from the short-lived T_x and T_y sublevels to the longer-lived T_z sublevel. The transition is observed as a decrease in the fluorescence signal, as the molecule is shelved for a longer period in the triplet state. The resonance line shapes of the electronic spin levels are asymmetric due to hyperfine interactions with nuclear spins (hydrogen, deuterium and carbon-13 atoms or other impurities).

gap between $T_x - T_z$ (see schematic in Figure 1.7b). Even though ODMR experiments allowed in-depth study of triplet states on single molecules, an all-optical approach, where the molecule is excited into the triplet from the ground state, remains to be demonstrated. In Chapter 6, I will discuss the theoretical and experimental framework of such an experiment.

1.2. OUTLINE OF THE THESIS

Although many host/guest systems have been studied in the past, the continuous exploration of new host matrices for guest molecules, such as the molecules shown in Figure 1.1, may lead to a better understanding of the modified properties of a guest molecule inside a host matrix. In these new systems, surprising effects can occasionally emerge. In the case of Chapter 2, a new host matrix is studied for (perdeuterated) perylene, namely dibenzothiophene. In this host matrix, a novel effect for single molecules was found in the form of reverse intersystem crossing, which was never observed before for (near) lifetime-limited linewidths. This effect allows for the tuning

of the photoblinking of the single molecule and the enhancement of the fluorescence signal.

The studies on this new host matrix for perylene are continued in Chapter 3. In that Chapter, we recorded the phosphorescence spectrum of perylene in order to find the energy of the triplet state. As the approximate location of the triplet state is known from the phosphorescence spectrum, an all-optical scheme, comparable to the discussed ODMR experiments, can be used to manipulate spin states in (and outside) a single molecule. The first attempts that we have performed to this end will be covered in Chapter 6.

In Chapter 4, we study another organic host matrix for single terrylene molecules. In this host matrix we observe a moderate linear Stark effect. As the mapping of electric fields, by use of the Stark effect, can be complicated by inhomogeneities in the coupling strength from molecule to molecule, we employ a method to deduce the dipole vector for each molecule individually. In addition, we use our measurements to propose a possible insertion of terrylene in the host matrix by use of quantum chemistry models.

Finally, in Chapter 5, we study an unconventional host matrix for single molecules, namely the two-dimensional material hexagonal boron nitride (hBN). With molecules on the surface of this host, we have shown for the first time that it is possible to record narrow zero-phonon lines of single molecules on a surface, rather than in the bulk of a host crystal. Our studies on hBN, which possesses much higher phonon energies than typical organic matrices, may make it in future possible to suppress linewidth broadening by temperature. Moreover, this host material may, unlike organic matrices, be applicable to a large variety of guest molecules.

REFERENCES

(1) Shpol'skii, E. *Doki. Akad. Nauk SSSR* **1952**, *87*.

(2) Shpol'skiĭ, É. V. *Soviet Physics Uspekhi* **1960**, *3*, 372.

(3) Moerner, W. E.; Kador, L. *Physical Review Letters* **1989**, *62*, 2535–2538.

(4) Orrit, M.; Bernard, J. *Physical Review Letters* **1990**, *65*, 2716–2719.

(5) Reinhardt, S. C. M.; Masullo, L. A.; Baudrexel, I.; Steen, P. R.; Kowalewski, R.; Eklund, A. S.; Strauss, S.; Unterauer, E. M.; Schlichthaerle, T.; Strauss, M. T.; Klein, C.; Jungmann, R. *Nature* **2023**, *617*, 711–716.

(6) Toninelli, C.; Gerhardt, I.; Clark, A. S.; Reserbat-Plantey, A.; Götzinger, S.; Ristanović, Z.; Colautti, M.; Lombardi, P.; Major, K. D.; Deperasińska, I.; Pernice, W. H.; Koppens, F. H. L.; Kozankiewicz, B.; Gourdon, A.; Sandoghdar, V.; Orrit, M. *Nature Materials* **2021**, DOI: 10.1038/s41563-021-00987-4.

(7) Basché, T.; Kummer, S.; Bräuchle, C. *Nature* **1995**, *373*, 132–134.

(8) Nicolet, A. A. L.; Hofmann, C.; Kol'chenko, M. A.; Kozankiewicz, B.; Orrit, M. *ChemPhysChem* **2007**, *8*, 1215–1220.

(9) Zirkelbach, J.; Mirzaei, M.; Deperasińska, I.; Kozankiewicz, B.; Gurlek, B.; Shkarin, A.; Utikal, T.; Götzinger, S.; Sandoghdar, V. *The Journal of Chemical Physics* **2022**, *156*, 104301.

(10) Kasha, M. *Discussions of the Faraday Society* **1950**, *9*, 14–19.

(11) Dunlop, D.; Ludvíková, L.; Banerjee, A.; Ottosson, H.; Slanina, T. *Journal of the American Chemical Society* **2023**, *145*, 21569–21575.

(12) Schofield, R. C.; Burdekin, P.; Fasoulakis, A.; Devanz, L.; Bogusz, D. P.; Hoggarth, R. A.; Major, K. D.; Clark, A. S. *ChemPhysChem* **2022**, *23*, e202100809.

(13) Lombardi, P.; Colautti, M.; Duquennoy, R.; Murtaza, G.; Majumder, P.; Toninelli, C. *Applied Physics Letters* **2021**, *118*, 204002.

(14) Basché, T.; Kummer, S.; Bräuchle, C. *Chemical Physics Letters* **1994**, *225*, 116–123.

(15) Schädler, K. G.; Ciancico, C.; Pazzagli, S.; Lombardi, P.; Bachtold, A.; Toninelli, C.; Reserbat-Plantey, A.; Koppens, F. H. L. *Nano Letters* **2019**, *19*, 3789–3795.

(16) Moradi, A.; Ristanović, Z.; Orrit, M.; Deperasińska, I.; Kozankiewicz, B. *ChemPhysChem* **2019**, *20*, 55–61.

(17) Faez, S.; van der Molen, S. J.; Orrit, M. *Physical Review B* **2014**, *90*, 205405.

(18) Clear, C.; Schofield, R. C.; Major, K. D.; Iles-Smith, J.; Clark, A. S.; McCutcheon, D. P. S. *Physical Review Letters* **2020**, *124*, 153602.

(19) Trebbia, J.-B.; Deplano, Q.; Tamarat, P.; Lounis, B. *Nature Communications* **2022**, *13*, 2962.

(20) Kiefer, W.; Rezai, M.; Wrachtrup, J.; Gerhardt, I. *Applied Physics B* **2016**, *122*, 38.

(21) Colautti, M.; Piccioli, F. S.; Ristanović, Z.; Lombardi, P.; Moradi, A.; Adhikari, S.; Deperasinska, I.; Kozankiewicz, B.; Orrit, M.; Toninelli, C. *ACS Nano* **2020**, *14*, 13584–13592.

(22) Tian, Y.; Navarro, P.; Orrit, M. *Physical Review Letters* **2014**, *113*, 135505.

(23) Esteso, V.; Duquennoy, R.; Ng, R.; Colautti, M.; Lombardi, P.; Arregui, G.; Chavez-Angel, E.; Sotomayor-Torres, C.; Garcia, P.; Hilke, M.; Toninelli, C. *PRX Quantum* **2023**, *4*, 040314.

(24) Phillips, W. A. *Reports on Progress in Physics* **1987**, *50*, 1657.

(25) Fleury, L.; Zumbusch, A.; Orrit, M.; Brown, R.; Bernard, J. *Journal of Luminescence* **1993**, *56*, 15–28.

(26) De Graaf, S. E.; Faoro, L.; Ioffe, L. B.; Mahashabde, S.; Burnett, J. J.; Lindström, T.; Kubatkin, S. E.; Danilov, A. V.; Tzalenchuk, A. Y. *Science Advances* **2020**, *6*, eabc5055.

(27) Lawetz, V.; Orlandi, G.; Siebrand, W. *The Journal of Chemical Physics* **1972**, *56*, 4058–4072.

(28) Schmidt, J.; Veeman, W. S.; van der Waals, J. H. *Chemical Physics Letters* **1969**, *4*, 341–346.

(29) Köhler, J.; Brouwer, A. C.; Groenen, E. J.; Schmidt, J. *Science (New York, N.Y.)* **1995**, *268*, 1457–1460.

(30) Wrachtrup, J.; Gruber, A.; Fleury, L.; von Borczyskowski, C. *Chemical Physics Letters* **1997**, *267*, 179–185.

(31) Brouwer, A. C. J.; Köhler, J.; Groenen, E. J. J.; Schmidt, J. *The Journal of Chemical Physics* **1996**, *105*, 2212–2222.